Journal of the Australian Ceramic Society (2018) 54:655–662
https://doi.org/10.1007/s41779-018-0194-3

RESEARCH

Fabrication and characterization of ZrO_2/Ni composites

Justyna Zygmuntowicz[1] · Pawel Falkowski[2] · Aleksandra Miazga[1] · Katarzyna Konopka[1]

Received: 22 May 2017 / Revised: 16 March 2018 / Accepted: 10 April 2018 / Published online: 5 May 2018

Abstract
This paper focuses on a research on the influence of nickel content in zirconia matrix and its impact on the mechanical properties of obtained composites. ZrO_2/Ni mixed powders were uniaxially pressed and sintered in a nitrogen atmosphere to obtain ZrO_2/Ni composites that were characterized by X-ray diffraction (XRD), scanning electron microscope (SEM), and energy-dispersive X-ray spectroscopy (EDS). The stereological analysis allows obtaining information about the size distribution of zirconia grains in the sintered composites. Relative density, hardness, fracture toughness, and bending strength were also analyzed. The results revealed that the presence of Ni particles in the composites affects the mechanical properties of the materials. An increased Ni concentration caused a decrease in Vickers hardness and increased the fracture toughness of the ZrO_2/Ni composites compared to the ZrO_2 samples. This kind of composite is of interest for temperature and flow sensors, thermal barrier coatings for gas turbines and supersonic propulsion systems of spacecrafts, as well as as a material for anode in solid oxide fuel cell.

Keywords Pressing · Composites · Mechanical properties · ZrO_2 · Nickel

Introduction

Nowadays, there is a lot of research on joining a brittle ceramic with microparticles of ductile metals. This is due to the interesting properties of this group of materials, such as high hardness, dissipation of most thermal stresses, and modification of thermal and electric properties [1, 2]. Furthermore, the presence of the reinforcing phase can prohibit the crack propagation and improve the fracture toughness of ceramics [3]. An example of ceramic-metal composite is ZrO_2-Ni composite. The zirconia-nickel system is a good candidate for a ceramic-metal composite because coefficients of thermal expansion of these components are very close to each other (13×10^{-6} K^{-1} for zirconia and 15×10^{-6} K^{-1} for nickel, respectively). This allows to minimize the stresses generated during sintering and facilities the formation of a good-quality interface between the phases without cracks and voids [4, 5]. Moreover, the elastic modulus of ZrO_2 and Ni is similar: 220 and 197 GPa, respectively. This system is very promising because zirconia and nickel are chemically stable and do not react with each other over a wide range of temperatures [6, 7]. According to the literature reports, this composite can be applied as thermal barriers, as sensor, and as anode for solid oxide fuel cells [8, 9]. The potential application of such materials is the reason for continuing work on this composite system carried out by many research centers [10–12].

This paper was focused on the influence of the nickel content on the microstructure of the ZrO_2 matrix. Two different metal contents were used in the experiments. In the work, the two commercially available powders were used. The samples were examined using X-ray diffraction (XRD), scanning electron microscope (SEM), energy-dispersive X-ray spectroscopy (EDS), and stereological analysis. Moreover, the hardness, fracture toughness, and bending strength were analyzed.

Experimental

The materials used in the experimental study were ZrO_2 TZ-PX-245 (TOSOH) with average grain size of 0.1 μm, purity of 99.9% and Ni particles (Sigma-Aldrich) with average size of a mean particle size of 4 μm, purity 99.9%. The zirconia powder was stabilized by 3 mol% Y_2O_3. The properties of the starting materials are shown in Table 1. The morphology of

✉ Justyna Zygmuntowicz
justyna.zygmuntowicz@inmat.pw.edu.pl

[1] Faculty of Materials Science and Engineering, Warsaw University of Technology, 141 Woloska Str, 02-507 Warsaw, Poland

[2] Faculty of Chemistry, Warsaw University of Technology, 3 Noakowskiego Str, 00-664 Warsaw, Poland

Table 1 Properties of the starting materials

Properties	Mean particle size from SEM investigation	Density from helium pycnometer	Melting point	Modulus of elasticity
	μm	g/cm^3	°C	GPa
ZrO_2	0.10 ± 0.03	5.93	2715	220
Ni	3.91 ± 2.15	8.90	1453	197

the powder particles was characterized by a scanning electron microscope (Fig. 1).

On the basis of SEM images, it was found that the starting Ni powder has an irregular shape. Moreover, the microscopic observation of started powders revealed that the ZrO_2 show the tendency to create agglomerates.

Three series of samples were prepared by die pressing: series I (100 vol.% ZrO_2), series II (85 vol.% ZrO_2 + 15 vol.% Ni), and series III (80 vol.% ZrO_2 + 20 vol.% Ni), respectively.

The preparation procedure of ceramic samples was as follows: mixing the ZrO_2 and Ni powders in a planetary ball mill (PM100, Retsch) in ethanol for 1 h, drying at 50 °C for 24 h, and shaping the samples by pressing operation. The 10 wt.% aqueous solution of poly(vinyl alcohol) (PVA) was used as a binder. The addition of the binder solution to the powders mixture was 10 wt.% with respect to weight of powder. The compacts with cylindrical shape with height of 3 mm and diameter of 20 mm were formed by uniaxial pressing at 100 MPa. The sintering was carried out at 1400 °C in a nitrogen atmosphere with 2 h of dwell time. The heating and cooling rate was 5 °C/min. The sintering temperature was chosen below the melting point of the Ni (1453 °C).

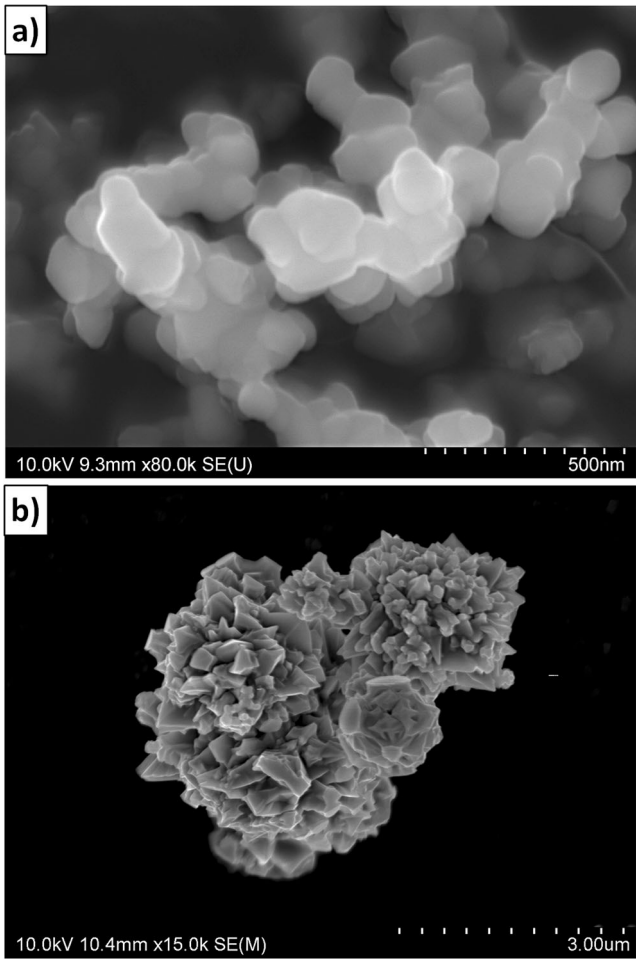

Fig. 1 Morphology of powders **a** ZrO_2 and **b** Ni

The bulk density of the sintered specimens was measured by Archimedes method in distilled water. Archimedes method was carried out according to the PN-76/6-06307. The measurements were made for 15 samples in each series. The densities of selected samples for each series were measured on a helium pycnometer, AccuPyc II 1340 (Micromeritics), in a sequence of 100 purges and 100 measurement cycles. The theoretical density was calculated according to the rule of mixtures. The following densities were used: 5.93 g/cm^3 for ZrO_2 and 8.9 g/cm^3 for Ni.

The XRD study was performed to determine the bulk crystalline phases of the composites. It was conducted using a Rigaku MiniFlex II diffractometer with CuKα 1.54 (λ = 1.54178 Å). The XRD conditions of recording were the following: voltage 30 kV, current 15 mA, angular range 2θ 25°–70°, step 0.02°, and counting time 0.5 s on the surface of samples from all series. The results were obtained in the form of plots of the diffracted intensities as a function of 2θ.

The fractures of samples were analyzed by scanning electron microscopy (HITACHI SU-70). The changes of size distribution of the ZrO_2 grains in the sintered composites were determined using a stereological analysis. A quantitative description of the microstructure was based on results of image analysis made by a Micrometer software [13]. The analysis was conducted on SEM micrographs of randomly selected areas positioned on a cross section of the sample. Before the measurements, the cross sections were polished and thermally etched. Polished surfaces for SEM observations were prepared by grinding and polishing with diamond pastes and silica suspension. The thermal etching was conducted at 1300 °C for 30 min. A thermal etching was adopted in the present study to reveal the grain boundaries of the zirconia matrix.

The local chemical composition was examined in areas on a fracture of the sample by EDS analysis (HITACHI SU-70 and SEM Zeiss Ultra Plus).

Moreover, the hardness was measured on a Vickers hardness tester (HVS-30T, Huatec Group Corporation) for sintered and polished samples. The hardness was determined by used means of a Vickers indenter with a load of 98.9 N with 10 s holding time. The corresponding indentation sizes were determined using an optical microscope (Nikon ECLIPSE LV150N). The fracture toughness K_{IC} was estimated using the crack length generated by an indenter using the Niihara equation [14]:

$$K_{IC} = 0.018 \cdot Hv^{0.6} \cdot E^{0.4} \cdot 2al^{-0.5} \quad (1)$$

In the above equation, E is the Young's modulus, l is the average crack length [μm], a is the one half of the indent diagonal length [μm], and H_V the Vickers hardness.

The strength of the discs was determined by using a ball-on-ring (BOR) test with a universal testing machine Tinius Olsen H10KS [15–17]. Reported strengths represented the mean and standard deviation of at least 10 specimens. The values were computed using Kirstein and Woole's equation:

$$\sigma_{max} = \frac{3P(1-\upsilon)}{4\Pi t^2}\left[1 + 2ln\frac{a}{b} + \frac{(1-\upsilon)}{(1+\upsilon)}\left\{1-\frac{b^2}{2a^2}\right\}\frac{a^2}{R^2}\right] \quad (2)$$

In the above equation, P is the applied load [N], υ the Poisson's ratio of specimens (0.30), t the thickness of disk [m], a the radius of supporting ring [m], b the radius of ball (the region of uniform loading at the centre) [m], and R the radius of specimens [m].

Results and discussion

The preliminary macroscopic and microscopic observation of the sintered samples revealed no pores or cracks in their volume and on their surface. The typical microstructure of the ZrO_2/Ni composites (series II and III) is presented in Fig. 2. In the microstructure, the areas with light (white) color represent the nickel particles and with gray color represent the zirconia matrix. The result of the observation of the microstructure reveals that the obtained sintered composites are characterized by quite homogenous distribution of Ni particle in the volume of material. Based on Fig. 2, it was found that the nickel particles in both series indicate tendency to agglomerate. A problem of Ni particle agglomeration could be minimized if colloidal processing would be used for composite preparation. There are at least two possible ways to overcome this problem. First, a suspension of ZrO_2 powder with Ni particles in the presence of dispersing agents should be well mixed in ball mill and sonicated. In this technique, ethanol or other easily evaporating solvent should be used. After that, the suspension should be dried and pulverized. In such a way, dry, homogenous, and ready to die pressing mixture of ZrO_2 with Ni should be obtained. The second approach requires a preparation of aqueous slurry with high fraction of ceramic and metallic powder (above 45 vol.%). The slurry should be stable; hence, an addition of dispersing agents and other processing aids is required. During the mixing and sonication the Ni particles, as well as ZrO_2, particles should be deagglomerated. The prepared slurry could be used in slip casting method (or other casting methods) to obtain desired composite.

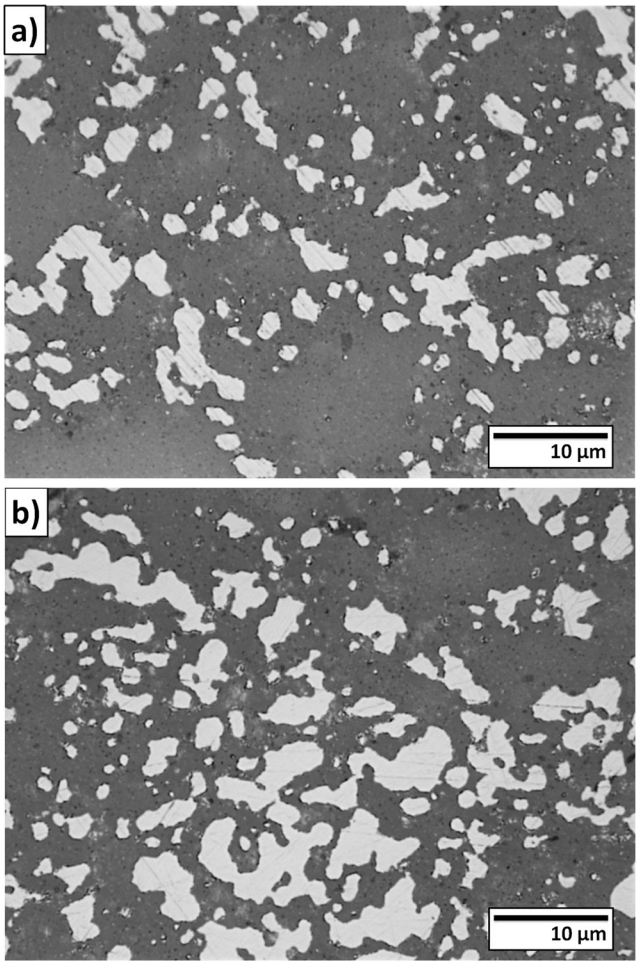

Fig. 2 Optical micrographs of the polished cross section of the zirconia-nickel composites **a** series II and **b** series III. –Nickel (bright contrast), zirconia (dark contrast)

Figure 3 shows the XRD patterns of the samples of each series after sintering. The XRD pattern for pure ZrO_2 (Fig. 3a) indicates materials containing tetragonal zirconia (t-ZrO_2) due to the addition of yttrium oxide. The X-ray diffraction patterns of composites indicate that the phase composition consists of tetragonal zirconia, nickel, nickel oxide, and monoclinic zirconia (m-ZrO_2). It can be stated that there was no reaction between zirconia and nickel during the sintering process. The observation at high magnification did not indicate the presence of transient phases. The NiO phase was detected because of oxidation of Ni and diffusion of oxygen from zirconia to nickel. The oxidation of Ni surface was confirmed by

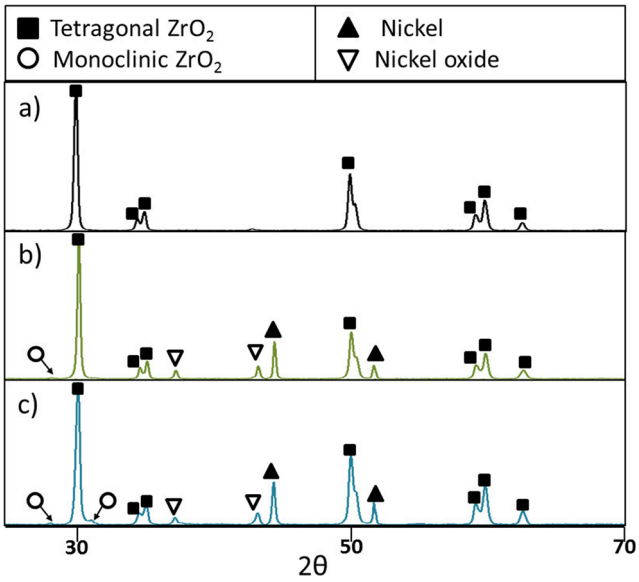

Fig. 3 X-ray diffraction analysis of the specimens **a** series I, **b** series II, and **c** series III

EDS analysis of a bulk nickel powder. The analysis revealed that the surface of Ni contains 1.41, 85.33, 0.46, and 12.80 atom % of oxygen, nickel, aluminum, and carbon, respectively. The presence of Al and C atoms on the surface may result from synthesis method [18] and the adsorption of carbon dioxide from air. The formation of small amount of NiO might have a positive effect on the composite properties. Duh and Chien [19] stated that bonding in Ni/zirconia (nickel foil to zirconia) required the formation of a thin oxide layer to wet the ceramics. That is why the presence of Ni-oxide should not compromise the properties of prepared composites.

For all samples, XRD spectra show an intensive characteristic peak of t-ZrO_2 at $2\theta = 30.2°$. For the composite samples, the research showed the presence of characteristic peaks of m-ZrO_2 at $2\theta = 28.2°$ and 31.5° with very weak intensity. At high nickel concentration, m-ZrO_2 peaks become more intensive which may indicate a higher content of this phase in the composite with the 20 vol.% of nickel. The effect of Ni addition on the t-m transformation of ZrO_2 during sintering in protective atmosphere (argon or reductive) is still not well recognized. More data could be found in the case of ZrO_2-NiO system. Danilenko et al. [10] concluded that the presence of Ni or NiO activated phase transformation toughening of zirconia by formation of metastable tetragonal phase depleted by Y^{3+} ions. The reversibly dissociation of NiO on Ni and oxygen in neutral (argon) atmosphere provided the formation of cubic phase and Y^{3+} depleted tetragonal phase. Internal oxidation of Ni during cooling leads to formation metastable tetragonal phase in depleted Y^{3+} zirconia grains. The formation of NiO particles during cooling leads to emergence of large compressive stresses, which also increased the metastability of tetragonal zirconia grains, depleted of Y^{3+} ions. In the case of synthesis of Ni-ZrO_2 via co-precipitation route, Elshazly et al. [20] observed that metastable t-ZrO_2 is stabilized at 20 mol% of nickel salt at a calcination temperature of 800 °C. Stefanic et al. [21] stated that the presence of NiO partially stabilizes the tetragonal polymorph of ZrO_2, but cannot stabilize the cubic polymorph of ZrO_2. Stabilization of the

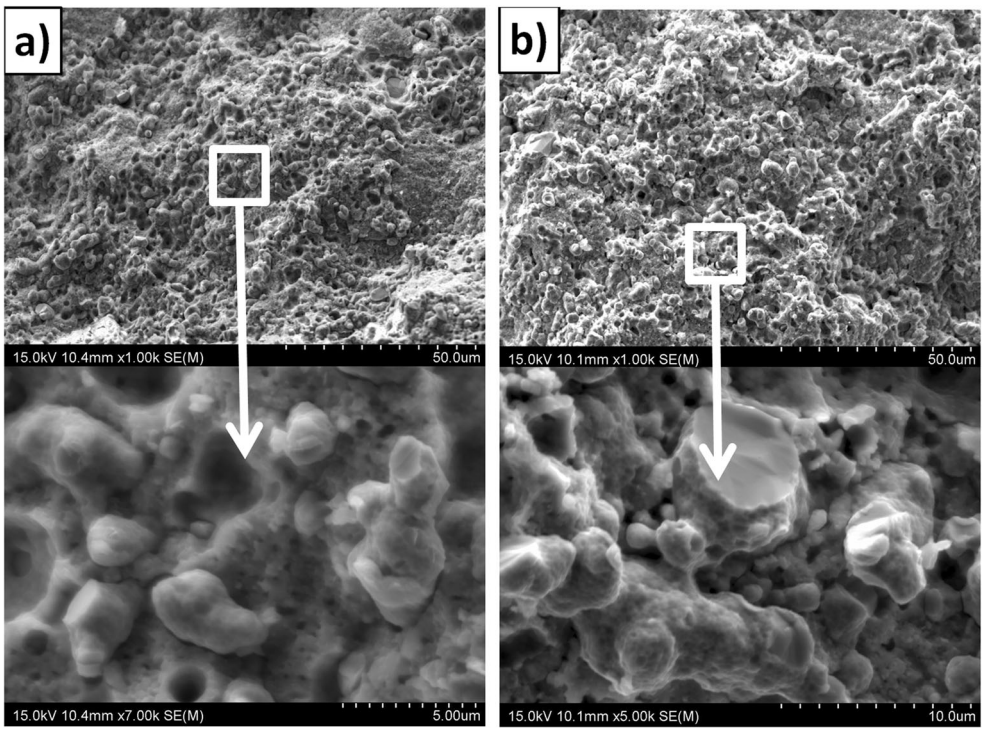

Fig. 4 Scanning electron micrographs of the samples **a** series II and **b** series III

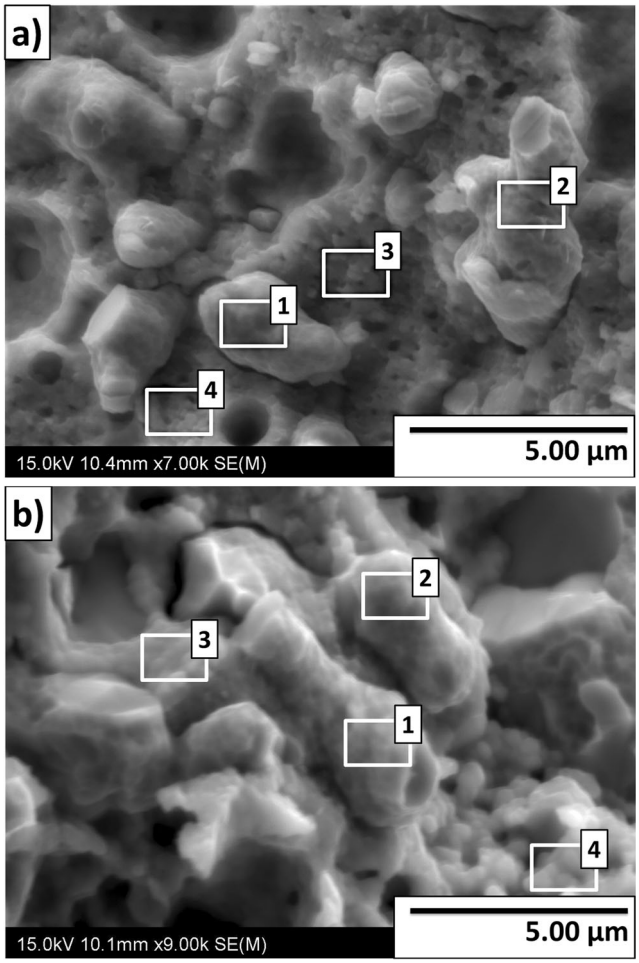

Fig. 5 Analysis of the chemical composition for selected areas on the fracture of ZrO_2-Ni composite **a** series II and **b** series III

t-ZrO_2-type phase rises with the increase in the NiO content up to 40 mol%. Stabilization of the t-ZrO_2-type phase in products with a NiO content above the solubility limit (5 mol% of Ni^{2+} ions) probably results from strong surface interactions between ZrO_2 and NiO.

Figure 4 shows the SEM images of the fracture surface of the ZrO_2/Ni composites of series II and III. There were no significantly differences between the fracture of both samples. These observations confirm that the nickel particles are uniformly distributed in the ceramic matrix. SEM observation reveals that most of the nickel particles are firmly bound to the ceramic matrix. For this reason, the presence of holes after pulled out of nickel particles was detected. It can be seen that the fracture of the Ni particles in the ZrO_2/Ni composite occurred mainly by cleavage, as shown in Fig. 4. There was no evidence of debonding at the particle/matrix interface.

The EDS analysis for selected areas on the fracture of the series II and series III was carried out. EDS spectra were collected from four different locations at a specimen. Areas used for making the measurement of EDS are shown in Fig. 5. The study was conducted on the fracture, so the tested surface is not flat, must take into account that the incident radiation can bounce back from the surface and can arouse adjacent elements. In addition, it should be remembered that on surface on the fracture, it may be a small amount of other phase which is invisible under microscope. The results of the concentration measurements of zirconium, nickel, oxygen, and yttrium in the composites of series II and III are presented in Table 2. The results showed that in the case of series II, not all of the nickel particles were oxidized to nickel oxide (area 1). In both series, the areas 1 and 2 contain mainly Ni. It also may be concluded that in series III, more nickel particles were oxidized to nickel oxide than in the case of series II. In these areas, probably nickel shows the tendency to rapid oxidation than series II and expected intensive diffusion in both direction Ni into ZrO_2 and ZrO_2 into Ni. The areas 3 and 4 in both

Table 2 The weight and atom content of samples from different areas

ZrO_2-Ni composites								
Series II—85 vol.% ZrO_2 + 15 vol.% Ni (Fig. 5a)								
Areas	Weight %				Atom %			
	Zr	Ni	O	Y	Zr	Ni	O	Y
Area 1	1.5 ± 0.1	96.7 ± 0.4	0	2.7 ± 0.1	0.9 ± 0.1	91.2 ± 0.4	0	7.9 ± 0.2
Area 2	2.0 ± 0.1	96.1 ± 0.4	0.7 ± 0.1	1.7 ± 0.1	1.2 ± 0.1	91.1 ± 0.4	2.5 ± 0.1	5.2 ± 0.2
Area 3	68.1 ± 0.3	19.0 ± 0.5	11.0 ± 0.1	1.8 ± 0.2	39.1 ± 0.2	16.9 ± 0.5	36.0 ± 0.4	8.0 ± 0.4
Area 4	61.1 ± 0.2	4.0 ± 0.2	32.9 ± 0.2	2.1 ± 0.1	22.6 ± 0.1	2.3 ± 0.1	69.3 ± 0.4	5.8 ± 0.2
Series III—80 vol.% ZrO_2 + 20 vol.% Ni (Fig. 5b)								
	Weight %				Atom %			
	Zr	Ni	O	Y	Zr	Ni	O	Y
Area 1	10.3 ± 0.2	83.8 ± 0.6	2.4 ± 0.1	3.5 ± 0.2	5.8 ± 0.1	73.3 ± 0.5	7.6 ± 0.4	13.3 ± 0.5
Area 2	3.4 ± 0.1	93.4 ± 0.7	0.4 ± 0.1	2.7 ± 0.1	2.0 ± 0.1	86.0 ± 0.6	1.4 ± 0.3	10.6 ± 0.5
Area 3	52.7 ± 0.3	16.4 ± 0.4	26.9 ± 0.3	3.9 ± 0.1	20.2 ± 0.1	9.7 ± 0.2	58.9 ± 0.6	11.1 ± 0.3
Area 4	60.1 ± 0.3	4.2 ± 0.3	32.1 ± 0.3	3.6 ± 0.1	21.8 ± 0.1	2.4 ± 0.2	66.4 ± 0.6	9.5 ± 0.3

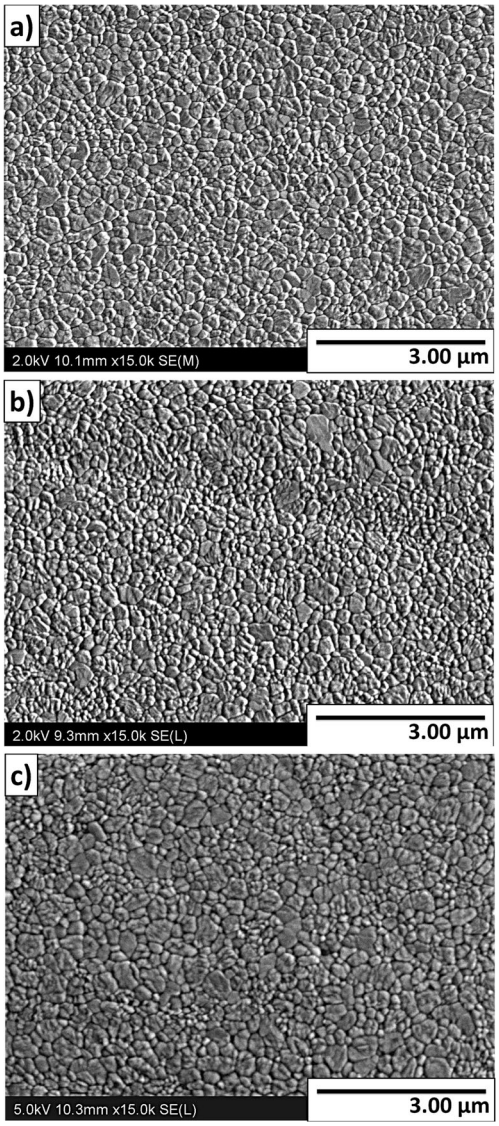

Fig. 6 SEM micrographs of particle size of ZrO_2 in **a** series I, **b** series II, and **c** series III, specimens after thermal etching

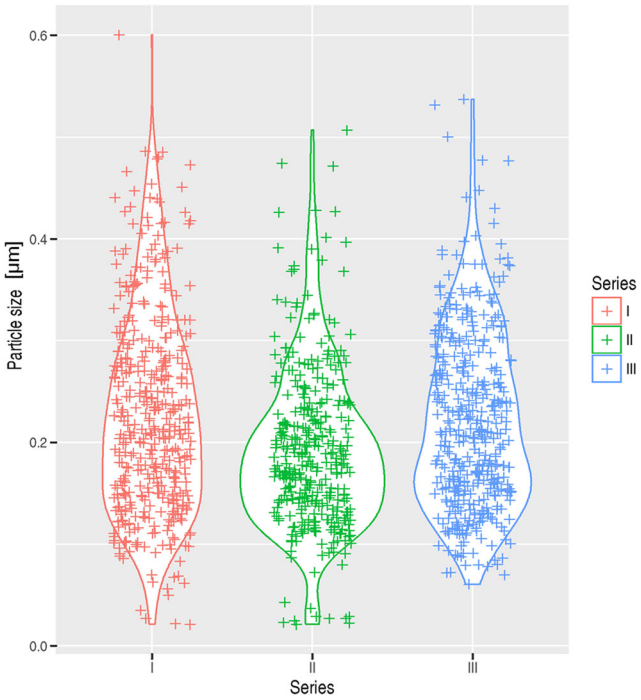

Fig. 7 Violin plots of the ZrO_2 particle size after thermal etching (series I, II, III)

series are rich in ZrO_2 and low amount of the nickel. The low amount of nickel in these areas is due to mutual diffusion of Zr to Ni and Ni contrary to the ZrO_2 matrix. These results showed that all areas contain yttrium. This is due to the fact that zirconia powder was stabilized by 3 mol% Y_2O_3 addition [22].

Figure 6 shows the microstructures of specimen matrix after thermal etching. In order to avoid a grain coarsening during thermal etching, the heating temperature was lowered by 100° than sintering temperature. The thermal etching at 1300 °C successfully reveals the grain boundaries of the matrix. Although some pores were identified occasionally, dense and relatively uniform microstructures were achieved, consistent with the measured densities shown in Table 3.

The size distribution of zirconia grains in the sintered composites is presented in the form of the violin plots in Fig. 7. The description of the grain size of the ZrO_2 was made on the basis of SEM images of randomly selected areas (in the case of series II and III, the nickel particles were neglected) on the samples using computer image analysis applying the program Micrometer [13]. This method allows obtaining information about the actual size of grains. Microstructure observations were performed using magnification ×15,000. The average values were calculated from measurement of 10 different areas.

Analysis of violin plots (Fig. 7) showed that the majority of grains in the samples of the series I have the size in the range from 0.1 to 0.3 µm. In the case of series II, most grains are in the range between 0.1 and 0.25 µm. The grain size in the

Table 3 Selected physical properties of specimens

Property		Series I (100 vol.% ZrO_2)	Series II (85 vol.% ZrO_2 + 15 vol.% Ni)	Series III (80 vol.% ZrO_2 + 20 vol.% Ni)
Theoretical density (calculated)	g/cm^3	5.93	6.37	6.52
Apparent density (Archimedes method)	g/cm^3	5.78	6.28	6.10
Relative density	%	97.60	98.60	93.50
Open porosity	%	1.6	0.5	0.9

Table 4 Selected mechanical properties of specimens

Sample	Hardness HV_{10} (GPa)	Fracture toughness (MPa $m^{0.5}$)	Bending strength (MPa)
ZrO_2	9.8	5.30 ± 0.30	425 ± 18
ZrO_2 + 15 vol.% Ni	7.1	6.03 ± 0.37	472 ± 44
ZrO_2 + 20 vol.% Ni	6.9	6.35 ± 0.33	421 ± 57

samples of series III varied between 0.1 and 0.35 μm. The obtained results allowed to calculate an average grain size in each series of samples, which were as follows: 0.23 ± 0.09, 0.19 ± 0.08, and 0.22 ± 0.09 μm for the series I, II, and II, respectively. It can be considered that the differences in the size distribution of ZrO_2 grains are not significant and the grain size distribution is quite uniform in the range 0.1–0.4 μm. Thereby, it can be stated that the addition of nickel particles does not influence the microstructure of ZrO_2 matrix.

The selected physical properties of the sintered samples are displayed in Table 3. It was found that the measured density of sinters was lower than the theoretical density. This indicates that the samples are characterized by some porosity. According to literature data, the optimal sintering temperature (relative density of samples close to theoretical) for the zirconia powder used for research is 1450 [23]. The used temperature was slightly lower which could cause a decrease in density. It may be seen that ZrO_2-15vol.% Ni composites had slightly higher density than pure zirconia. Higher content of metallic phase in composite (20 vol.%) caused a decrease in density. This may result from the hindered homogenization of the starting powders prior to pressing, which could have resulted in a larger amount of powder agglomerates which, after sintering, increased the porosity. Furthermore, with a higher content of nickel powder in the final composite, the nickel oxide content also increased. NiO phase has a lower density than nickel ($\rho_{NiO} = 6.67$ g/cm^3) which also can influenced the densification. In series II, the open porosity is 0.5%, while in series III, the open porosity slightly increases and is 0.9%.

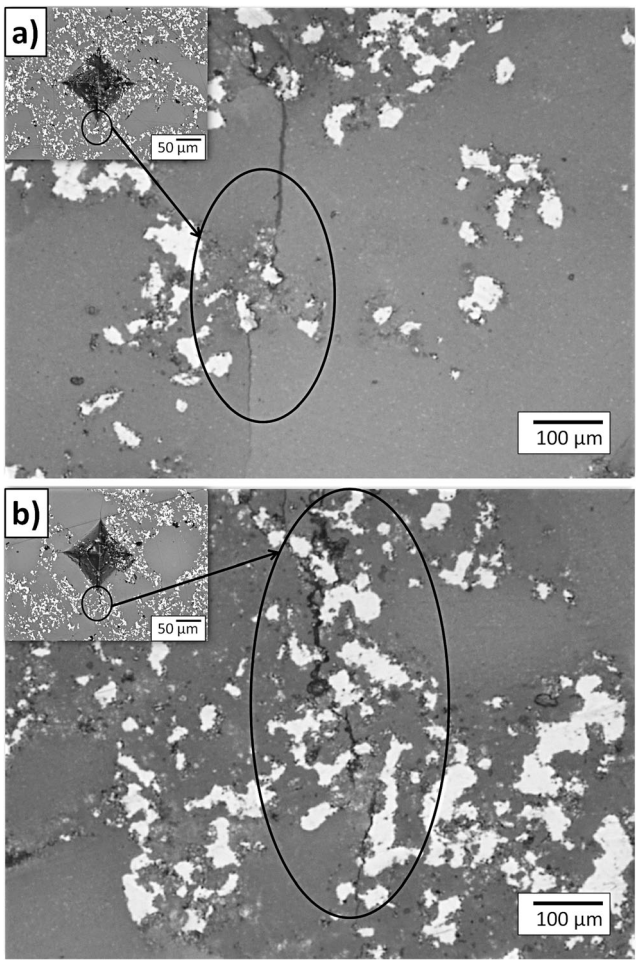

Fig. 8 The optical micrographs showing the examples of Vickers indentation in the sintered samples **a** series II and **b** series III

Due to the addition of metal particles into ceramic matrix, the Vickers hardness of the series II and III was decreased in comparison to the hardness of the series I. The addition of the 15 and the 20 vol.% of metallic phase caused the decrease of hardness by 27 and 29%, respectively, compared to a sample made of pure ZrO_2 (series I).

The density of sintered composites also has an influence on bending strength (Table 4). The composites made of the ZrO_2 and 15 vol.% Ni, that shows the highest relative density, also exhibit the best mechanical properties. Although the bending strength of samples from the series I and the series III is similar, a standard deviation and a coefficient of variation of the series III are higher (standard deviation of series I and III is 18 and 57, respectively, while the coefficient of variation of the series I and III is 0.04 and 0.14, respectively). Hence, it can be assumed that samples made of pure ZrO_2 show higher homogeneity in comparison to ZrO_2 and 20 vol.% Ni composites.

One of the most important parameters for ceramic matrix composites is fracture toughness. The present study has shown that the addition of nickel (series II and series III) improves the fracture toughness in comparison to a sample made of ZrO_2. For the samples of the series I, the K_{1c} values are close to 5.30 MPa $m^{0.5}$. It was observed that in the case of the samples made of ZrO_2 and 15 vol.%, Ni fracture toughness is higher (6.03 MPa $m^{0.5}$) than for the series I. The increase in values of K_{1c} is also achieved for the series III (6.35 MPa $m^{0.5}$).

Figure 8 shows an example of crack propagation on the polished cross section of the ZrO_2/Ni composites after the Vickers indentation. It can be seen that the deflection of the crack propagation is caused by the presence of Ni particles. The crack propagates smoothly in the ceramic matrix and on

intercepting the metal particles follow the ZrO_2/metal interface. It was found that in the case of the series III, in which the elongated nickel particles are present, the crack also passes through the nickel particle. Two types of toughening mechanisms, crack deflection and crack bridging, are observed for the nickel particles in the composite.

Conclusions

Results showed that the presence of Ni particles in the composites has an influence on the mechanical properties. An increased Ni concentration decreases Vickers hardness and increases the fracture toughness of the ZrO_2/Ni composites compared with the samples made of ZrO_2. Two types of toughening mechanisms are responsible for the high fracture toughness: crack deflection and crack bridging. What is more, a high content of Ni in composites inhibits the densification process, so the samples with the 20 vol.% of Ni show lower relative densities and higher porosity. The addition of the 15 vol.% of Ni increases the bending strength. For higher content of Ni, the bending strength decreases, but it must be noticed that the mechanical strength is strongly dependant from density and porosity of measured samples. It is possible that for the similar relative densities of composites with different content of Ni particles, the samples with higher amount of Ni will have a higher bending strength. However, these assumptions required further investigations.

The present study has also shown that the addition of Ni particles up to the 20 vol.% does not influence on a grain growth of ZrO_2 during sintering process.

XRD analysis of composites showed that there was no reaction between zirconia and nickel during the sintering process. The NiO phase was detected due to oxidation of Ni and diffusion of oxygen from zirconia to nickel.

Acknowledgements This work was supported by the Faculty of Material Science and Engineering Warsaw University of Technology (statute work).

References

1. Sigl, L.S., Mataga, P.A., Dalgleish, B.J., McMeeking, R.M., Evans, A.G.: On the toughness of brittle materials reinforced with a ductile phase. Acta Metall. **36**(4), 945–953 (1988)
2. Rodriguez-Suarez, T., Bartolome, J.F., Moya, J.S.: Mechanical and tribological properties of ceramic/metal composites: a review of phenomena spanning from the nanometer to the micrometer length scale. J Eur Ceram Soc. **32**, 3887–3898 (2012)
3. Konopka, K., Maj, M., Kurzydłowski, K.J.: Studies of the effect of metal particles on the fracture toughness of ceramic matrix composites. Mater Charact. **51**(5), 335–340 (2003)
4. Beltran, J.I., Gallego, S., Cerdá, J., Moya, J.S., Muñoz, M.C.: Bond formation at the Ni/ZrO_2 interface. Phys Rev B. **68**, 7–15 (2003)
5. Lopez-Esteban, S., Rodriguez-Suarez, T., Esteban-Betegon, F., Pecharroman, C., Moya, J.S.: Mechanical properties and interfaces of zirconia/nickel in micro- and nanocomposites. J Mater Sci. **41**, 5194–5199 (2006)
6. Morales-Rodriguez, A., Bravo-León, A., Domínguez-Rodríguez, A., López-Esteban, S., Moya, J.S., Jiménez-Melendo, M.: High-temperature mechanical properties of zirconia/nickel composites. J Eur Ceram Soc. **23**, 2849–2856 (2003)
7. Morales-Rodriguez, A., Bravo-León, A., Domínguez-Rodríguez, A., Jiménez-Melend, M.: High-temperature plastic behavior of TZP-Ni cermets. J Am Ceram Soc. **91**(2), 500–507 (2008)
8. Aruna, S.T., Muthuraman, M., Patil, K.C.: Synthesis and properties of Ni–YSZ cermet: anode material for solid oxide fuel cells. Solid State Ionics. **111**, 45–51 (1998)
9. Koide, H., Someya, Y., Yoshida, T., Maruyama, T.: Properties of Ni/YSZ cermet for SOFC. Solid State Ionics. **132**, 253–260 (2000)
10. Danilenko, I., Glazunov, F., Konstantinova, T., Yashchyshyn, I., Burkhovetski, V., Volkova, G.: Effect of Ni/NiO particles on structure and crack propagation in zirconia based composites. Adv Mater Lett. **5**(8), 465–471 (2014)
11. Gutierrez-Gonzalez, C.F., Solis Pinargote, N.W., Agouram, S., Peretyagin, P.Y., Lopez-Esteban, S., Torrecillas, R.: Spark plasma sintering of zirconia/nano-nickel composites. Mech Ind. **16**(7), 703 (2015)
12. Lopez-Esteban, S., Bartolome, J.F., Moya, J.S., Tanimoto, T.: Mechanical performance of 3Y-TZP/Ni composites: tensile, bending and uniaxial fatigue test. J Mater Res. **17**(7), 1592–1600 (2002)
13. Michalski, J., Wejrzanowski, T., Pielaszek, R., Konopka, K., Łojkowski, W., Kurzydłowski, K.J.: Application of image analysis for characterization of powders. Mater Sci Poland. **23**, 79–86 (2005)
14. Niihara, K.: A fracture mechanics analysis of indentation induced Palmqvist cracks in ceramics. J Mater Lett. **2**, 221 (1983)
15. With, G., Wagemans, H.H.: Ball-on-ring test revisited. J Am Ceram Soc. **72**, 1538–1541 (1989)
16. Chae SH, Zhao JH, Edwards DR, Ho PS. Verification of ball-on-ring test using finite element analysis. Therm Thermomech Phenom Electron Syst 2010;1–6
17. Shetty, D.K., Rosenfield, A.R., McGuire, P., Bansal, G.K., Duckworth, W.H.: Biaxial flexure tests for ceramics. Am Ceram Soc Bull. **59**, 551–553 (1980)
18. Jensen, H., Soloviev, A., Li, Z., Søgaard, E.G.: XPS and FTIR investigation of the surface properties of different prepared titania nano-powders. Appl Surf Sci. **246**, 239–249 (2005)
19. Duh, J.G., Chien, W.S.: Microstructural characteristics in Ni/zirconia bonding. J Mater Sci. **25**(3), 1529–1536 (1990)
20. Elshazly, S.E., Abdelal, O.A.A.: Nickel stabilized zirconia for SOFCs: synthesis and characterization. Int J Metall Eng. **1**(6), 130–134 (2012)
21. Štefanić, G., Didović, M., Musić, S.: The influence of thermal treatment on the phase development of ZrO2–NiO precursors. J Mol Struct. **834–836**, 435–444 (2007)
22. Chevalier, J., Gremillard, L., Virkar, A.V., Clarke, D.R.: The tetragonal-monoclinic transformation in zirconia: lessons learned and future trends. J Am Ceram Soc. **92**, 1901–1920 (2009)
23. Matsuzaki, F., Sekine, H., Honma, S., Takanashi, T., Furuya, K., Yajima, Y., Yoshinari, M.: Translucency and flexural strength of monolithic translucent zirconia and porcelain-layered zirconia. Dent Mater. **34**(6), 910–917 (2015)